J Inorg Organomet Polym (2016) 26:962–974
DOI 10.1007/s10904-016-0403-x

Synthesis and Characterization of Pure Phase Zn(II) and Cd(II) Oxide Nanoparticles via Thermal Decomposition of Four New Zn(II) and Cd(II) Coordination Polymers

Farzin Marandi[1] · Lida Hashemi[2] · Ali Morsali[2] · Harald Krautscheid[3]

Received: 5 March 2016 / Accepted: 27 June 2016 / Published online: 4 July 2016

Abstract Four new Zn(II) and Cd(II) coordination polymers, $[Zn(2\text{-}AMP)_2(N_3)_2]_n$ (**1**), $[Zn(2\text{-}AMP)_2(SCN)_2]_n$ (**2**), $[Cd(2\text{-}AMP)(N_3)_2]_n$ (**3**) and $[Cd(2\text{-}AMP)_2(SCN)_2]_n$ (**4**) {2-AMP: 2-Aminomethylpyridine}, have been synthesized and characterized by single crystal X-ray diffraction, IR spectroscopy and elemental analyses. The Zinc(II) oxide and Cadmium(II) oxide nano-particles have been synthesized from thermolysis of **1**–**4** at 600 °C under air atmosphere for 4 h. The ZnO and CdO nanoparticles were characterized by X-ray diffraction and scanning electron microscopy (SEM). SEM images show the average size of produced ZnO and CdO nanoparticles are 60–70 nm in all compounds.

Keywords Cadmium(II) coordination polymer · Zinc(II) coordination polymer · Nano-structures · Calcination

1 Introduction

The design of metal-coordination polymers are attracting interest due to their different topologies and applications in smart optoelectronic, magnetic, microporous, and biomimetic materials with specific structures, properties, and reactivities that are not found in mononuclear compounds, and because of these special characters they have been studied widely [1–10]. Organic ligands are very momentous in design a construction of desirable frameworks, since changes in flexibility, length and symmetry of organic ligands can lead to the formation of class of materials with different architectures and functions [1]. 2-Aminomethylpyridine is one of the N-donor ligands which have been used in modeling complexes to mimic the non-covalent interactions in biological processes. Controlling the growth of materials at the submicrometer scale is of central importance in the emerging field of nanotechnology [11–14]. The potential use of coordination polymers as materials for nano technological applications would seem to be very extensive. Nanometer-scaled materials often exhibit the new interesting size-dependent physical and chemical properties that cannot be observed in their bulk analogue. In this paper we report four new Zn(II) and Cd(II) coordination polymer with 2-Aminomethylpyridine ligands $[Zn(2\text{-}AMP)_2(N_3)_2]_n$ (**1**), $[Zn(2\text{-}AMP)_2(SCN)_2]_n$ (**2**), $[Cd(2\text{-}AMP)(N_3)_2]_n$ (**3**) and $[Cd(2\text{-}AMP)_2(SCN)_2]_n$ (**4**). ZnO is polar inorganic crystalline material with many applications due to their interesting properties such as nontoxicity, good electrical, optical and piezoelectric behavior, stability in a hydrogen plasma atmosphere and low price [15–24]. ZnO is a well-known semiconductor with a wide direct band gap (3.37 eV) and a large excitation binding energy of 60 meV at room temperature [18, 19]. It has a wide range of applications such as solar cells, luminescent, electrical and acoustic devices, gas and chemical sensors, coatings, catalysts, micro lasers, memory arrays and biomedical applications [20]. Till now, many methods have been developed to synthesis of zinc(II) oxide nanocrystals including vapor phase growth [21], vapor liquid-solid process [16], soft chemical method [23], electrophoretic deposition [24], sol–gel process [25, 26], homogeneous precipitation [27], etc. In other hand Cadmium

✉ Farzin Marandi
f.marandi@gmail.com

✉ Ali Morsali
morsali_a@modares.ac.ir

[1] Department of Chemistry, Payame Noor University, Tehran 19395-4697, Islamic Republic of Iran

[2] Department of Chemistry, Faculty of Sciences, Tarbiat Modares University, P.O. Box 14155-4838, Tehran, Islamic Republic of Iran

[3] Institut für Anorganische Chemie, Universität Leipzig, Johannisallee 29, 04103 Leipzig, Germany

oxide ($E_g \sim 2.3$ eV) is an n-type degenerate semiconductor with high electrical conductivity. Due to its large linear refractive index ($n_0 = 2.49$) it is a promising candidate for optoelectronic applications and other applications including solar cells, photo transistors, photodiodes, transparent electrodes and gas sensors [28, 29]. The use of coordination polymers as precursors for the provision of inorganic nanomaterials such as zinc(II) oxide and cadmium(II) oxide has not yet been investigated thoroughly. In this paper we describe a simple method for preparing nano-particles of ZnO and CdO by the use of $[Zn(2\text{-}AMP)_2(N_3)_2]_n$ (**1**), $[Zn(2\text{-}AMP)_2(SCN)_2]_n$ (**2**), $[Cd(2\text{-}AMP)(N_3)_2]_n$ (**3**) and $[Cd(2\text{-}AMP)_2(SCN)_2]_n$ (**4**) as a precursors.

2 Experimental

2.1 Materials and Physical Techniques

All reagents and solvents for the synthesis and analysis were commercially available and used as received. IR spectra were recorded using Perkin-Elmer and nicolet 510P spectrophotometers. X-ray powder diffraction (XRD) measurements were performed using an X'pert diffractometer of Philips Company with monochromated Cuk_α radiation ($\lambda = 1.54178$ Å). The nano samples were characterized with a scanning electron microscope (SEM) (Philips XL 30) with gold coating. Crystallographic measurements of compound **1** was made at 298(2) K using a Bruker APEXII CCD area detector diffractometer equipped with a graphite monochromated Mo-k_α radiation ($\lambda = 0.71073$ Å). The structure was solved by direct methods and refined by refinement of F^2 against all reflections. The molecular structure plots were prepared using ORTEPIII [30] and Mercury software [31].

2.2 Synthesis of $[Zn(2\text{-}AMP)_2(N_3)_2]_n$ (1)

Compound **1** was prepared using the following method: 2-AMP (1 mmol), Zinc(II) acetate (0.5 mmol) and NaN_3(1 mmol) were placed in the main arm of a branched tube. MeOH/EtOH 2:1 was carefully added to fill both arms. The tube was sealed and the ligand-containing arm immersed in an oil bath at 60 °C while the other arm was kept at ambient temperature. After 2–3 days crystals obtained and then filtered off and air dried. IR (selected bands; in cm^{-1}): 579 (w), 630 (w), 772 (s), 1017 (s), 1217(s), 1440 (s), 1590 (s), 2036 (vs), 3148 (m), 3263 (m).

2.3 Synthesis of $[Zn(2\text{-}AMP)_2(SCN)_2]_n$ (2)

Compound **2** was prepared using the following method: 2-AMP (1 mmol), Zinc(II) acetate (0.5 mmol) and KSCN (1 mmol) were placed in the main arm of a branched tube. MeOH/EtOH 2:1 was carefully added to fill both arms. The tube was sealed and the ligand-containing arm immersed in an oil bath at 60 °C while the other arm was kept at ambient temperature. After 2–3 days crystals obtained and then filtered off and air dried. IR (selected bands; in cm^{-1}): 553 (s), 649 (s), 771 (vs), 961 (s), 1270 (m), 1436 (s), 1590 (s), 2047 (vs), 3164 (w), 3248 (m).

2.4 Synthesis of $[Cd(2\text{-}AMP)(N_3)_2]_n$ (3)

Compound **3** was prepared using the following method: 2-AMP (1 mmol), cadmium(II) acetate (0.5 mmol) and NaN_3 (1 mmol) were placed in the main arm of a branched tube. MeOH/EtOH 2:1 was carefully added to fill both arms. The tube was sealed and the ligand-containing arm immersed in an oil bath at 60 °C while the other arm was kept at ambient temperature. After 2–3 days crystals obtained and then filtered off and air dried. IR (selected bands; in cm^{-1}): 539 (w), 653 (w), 770 (m), 1014 (m), 1285 (m), 1440 (m), 1603 (m), 2050 (vs), 3267 (w), 3310 (m).

2.5 Synthesis of $[Cd(2\text{-}AMP)_2(SCN)_2]_n$ (4)

Compound **4** was prepared using the following method: 2-AMP (1 mmol), cadmium(II) acetate (0.5 mmol) and KSCN (1 mmol) were placed in the main arm of a branched tube. MeOH/EtOH 2:1 was carefully added to fill both arms. The tube was sealed and the ligand-containing arm immersed in an oil bath at 60 °C while the other arm was kept at ambient temperature. After 2–3 days crystals obtained and then filtered off and air dried. IR (selected bands; in cm^{-1}): 539 (w), 629 (m), 757 (s), 1009 (vs), 1279 (w), 1436 (s), 1588 (m), 2067 (vs), 3249 (w), 3310 (w).

2.6 Synthesis of ZnO and CdO Nano-Structures

ZnO and CdO nano partiecles were prepared by direct thermolyses of compounds 1–4 at 600 °C under air atmosphere for 4 h.

3 Results and Discussion

Reaction of ligands 2-Aminomethylpyridine with Zinc(II) acetate and cadmium(II) acetate led to the formation of four Zn(II) and Cd(II) coordination polymers $[Zn(2\text{-}AMP)_2(N_3)_2]_n$ (**1**), $[Zn(2\text{-}AMP)_2(SCN)_2]_n$ (**2**), $[Cd(2\text{-}AMP)(N_3)_2]_n$ (**3**) and $[Cd(2\text{-}AMP)_2(SCN)_2]_n$ (**4**). The IR spectrum displays characteristic absorption bands for the both complexes. The IR absorption bands with a variable intensity in the frequency range 1205–1585 cm^{-1}

correspond to vibrations of the pyridine rings. *v* (aromatic CH) vibrations are found at around 3000 cm^{-1}. The ORTEP view with numbering scheme for compounds is shown in Figs. 1, 2, 5 and 6. Determination of the structure of compound **1** by X-ray crystallography (Table 1; Figs. 1, 3) showed that in the crystal structure of compound **1**, Zn^{II} is six-coordinate in a configuration by four nitrogen atoms from 2-Aminomethylpyridine

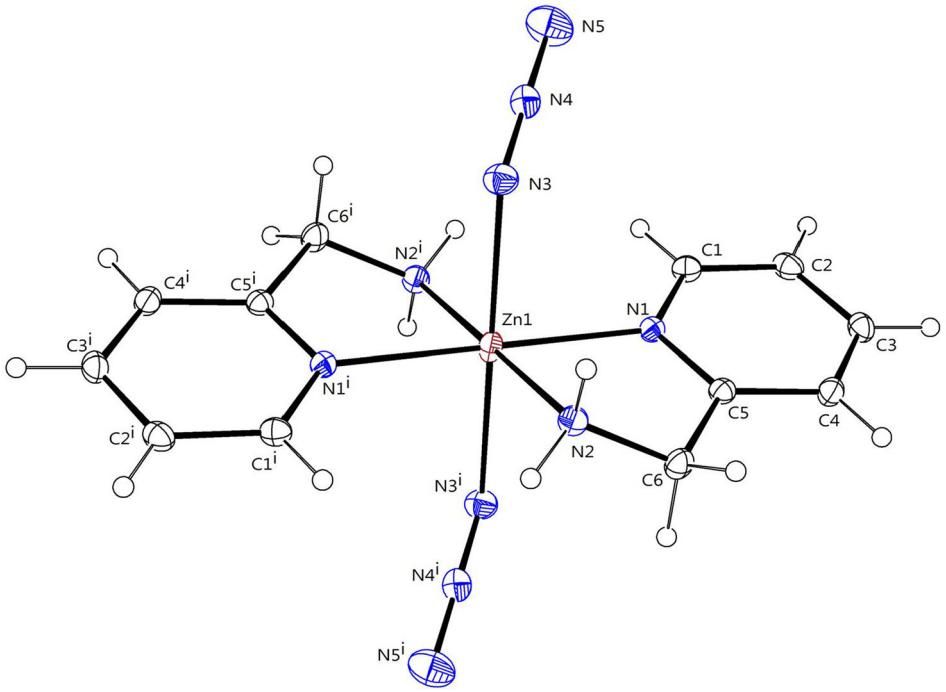

Fig. 1 ORTEP diagram of compound (**1**)

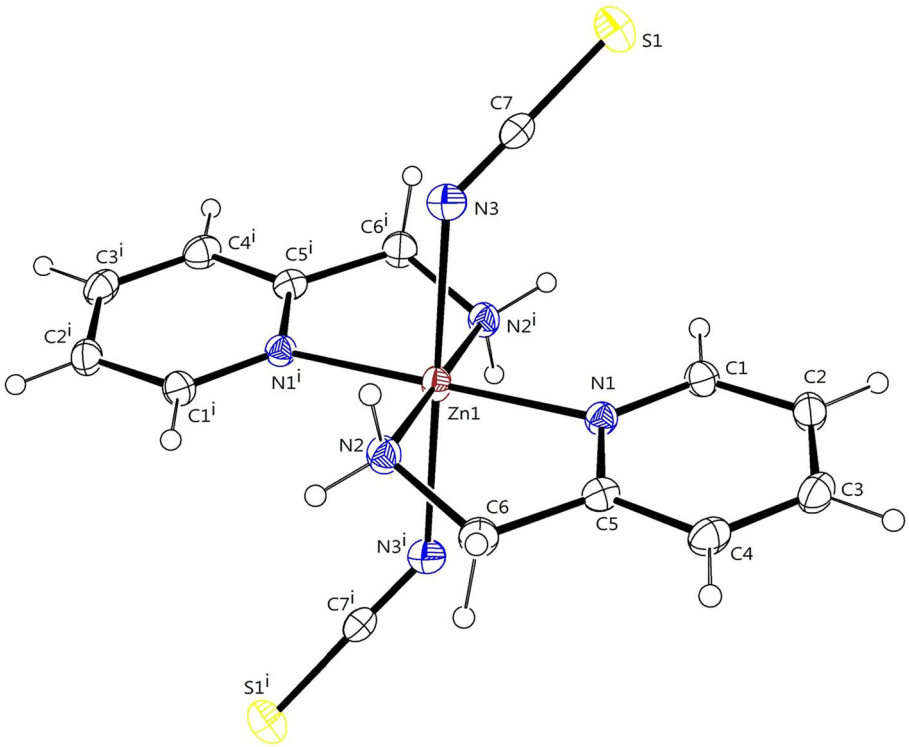

Fig. 2 ORTEP diagram of compound (**2**)

Table 1 Crystal data and structure refinement for **1–2**

	Zn–NNN(1)	Zn–NCS(2)
Identification code	$[Zn(amp)_2(N_3)_2]$	$[Zn(amp)_2(NCS)_2]$
Empirical formula	$C_{12}H_{16}N_{10}Zn$	$C_{14}H_{16}N_6S_2Zn$
Formula weight	365.72	397.82
Crystal system	Monoclinic	Monoclinic
Space group	P2(1)/c	P2(1)/c
Unit cell dimensions	$a = 8.7104$ (7) Å	$a = 9.2048$ (7) Å
	$b = 9.0842$ (5) Å	$b = 9.2915$ (6) Å
	$c = 9.3784$ (8) Å	$c = 9.7508$ (7) Å
	$\alpha = 90°$	$\alpha = 90°$
	$\beta = 94.14$ (1) °	$\beta = 93.342$ (9) °
	$\gamma = 90°$	$\gamma = 90°$
Volume	740.15(10) Å^3	832.53 (10) Å^3
Z	2	2
Density (calculated)	1.641 g cm^{-3}	1.578 g cm^{-3}
Absorption coefficient	1.676 mm^{-1}	1.733 mm^{-1}
F(000)	376	408
θ range for data collection	2.3 to 28.1	3.12 to 27.00
Index ranges	$-11 \leq h \leq 11$	$-11 \leq h \leq 11$
	$-11 \leq k \leq 11$	$-11 \leq k \leq 11$
	$-11 \leq l \leq 11$	$-12 \leq l \leq 12$
Reflections collected	7010	6551
Independent reflections	1719 [R(int) = 0.0369]	1820 [R(int) = 0.0318]
Completeness to theta	96.1 %	99.7 %
Data/restraints/parameters	1719/0/107	1820/0/106
Goodness-of-fit on F^2	1.042	0.943
Final R indices [I > 2sigma(I)]	R1 = 0.0246, wR2 = 0.0693	R1 = 0.0256, wR2 = 0.0647
indices (all data)	R1 = 0.0282, wR2 = 0.0701	R1 = 0.0308, wR2 = 0.0656
Largest diff. peak, hole	0.35, −0.26 e Å^{-3}	0.45, −0.20 e Å^{-3}

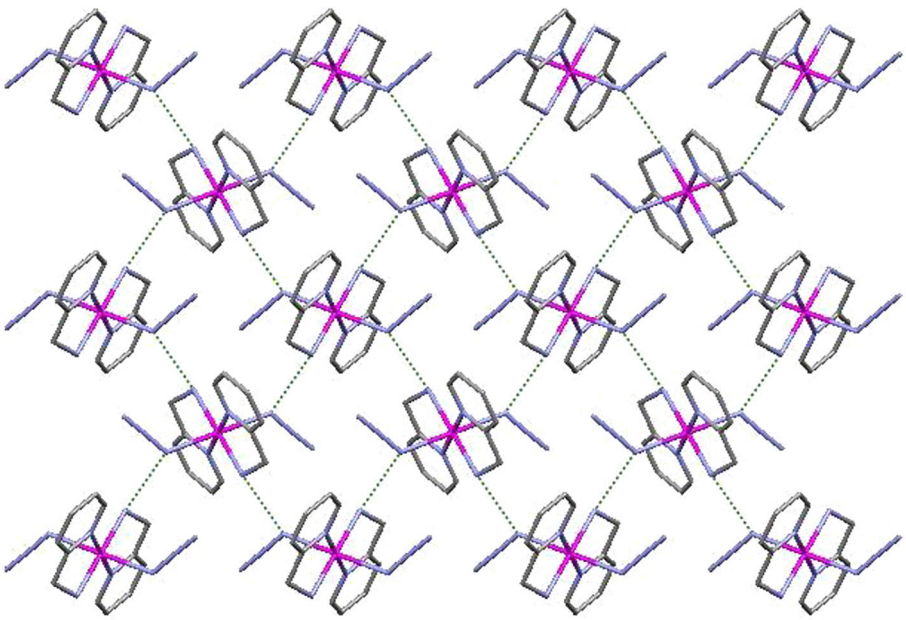

Fig. 3 The packing diagram of compound (**1**)

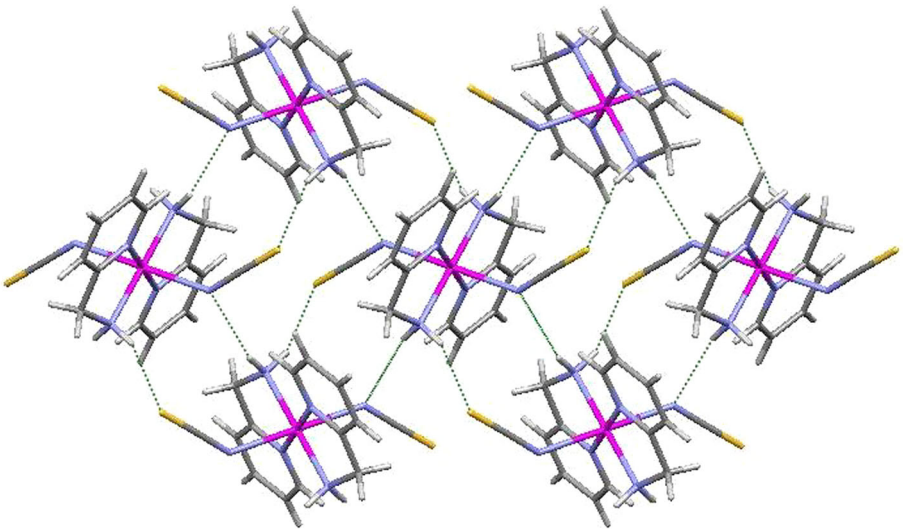

Fig. 4 The packing diagram of compound (**2**)

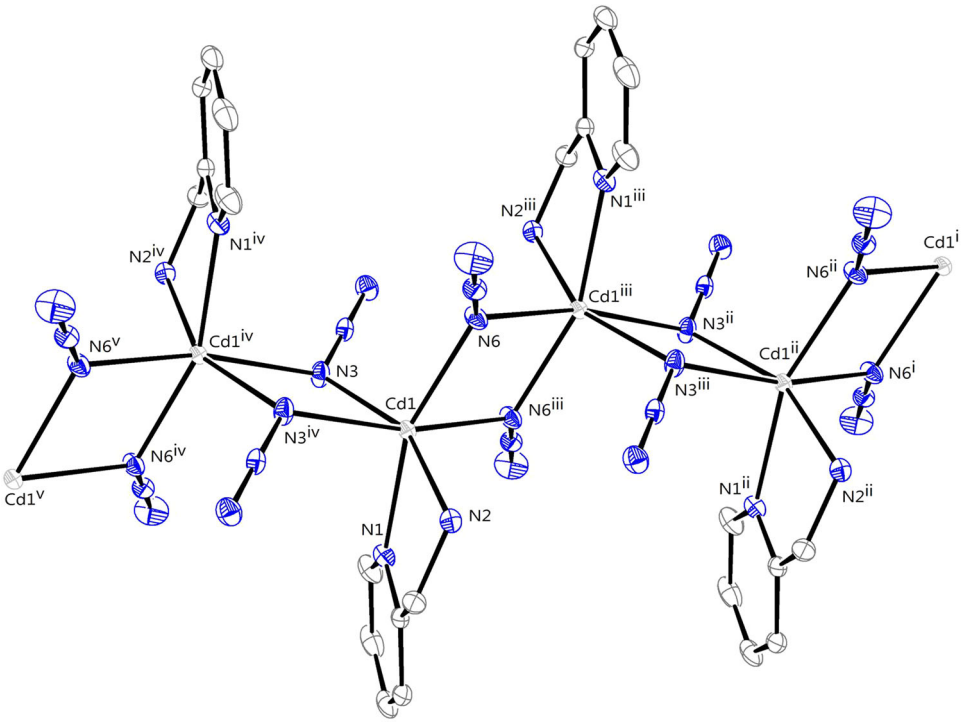

Fig. 5 ORTEP diagram of compound (**3**)

ligand and two nitrogen atoms from two N_3^- counter ion. Selected bond lengths/Å and angles/° and hydrogen bonding have been listed in for compound **1** respectively. In the crystal structure of **1**, Fig. 2, intermolecular C–H···N hydrogen bonds (Table 5), π-π interaction between the pyridine rings and other intermolecular interaction are effective in stabilization of the crystal structure and formation of the 3-D supramolecular complex. Selected bond lengths/Å and angles/° and hydrogen bonding have been listed in Table 3. Determination of the structure of compound **2** by X-ray crystallography (Table 1; Figs. 2, 4) showed that in the crystal structure of compound **1**, Zn^{II} is six-coordinate in a configuration by four nitrogen atoms from 2-Aminomethylpyridine ligand and two nitrogen atoms from two NCS^- counter ion. Selected bond lengths/Å and angles/° and hydrogen bonding have been listed in Tables 3 and 5 for compound **2** respectively. In the crystal structure of **2**, Fig. 4, intermolecular N–H···N, N–H···S and C–H···S hydrogen bonds (Table 5), π-π interaction between the pyridine rings and other

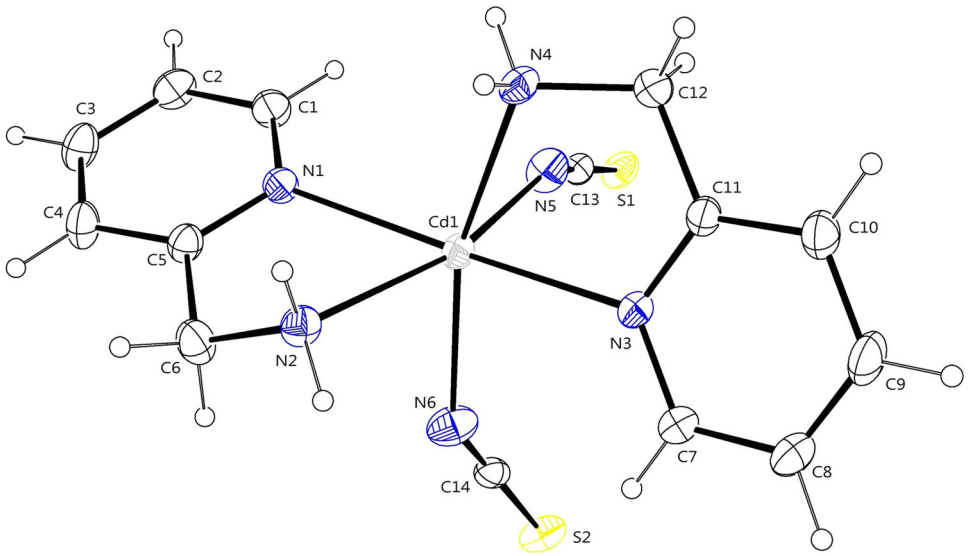

Fig. 6 ORTEP diagram of compound (**4**)

Table 2 Crystal data and structure refinement for **3**–**4**

	Cd–NNN(3)	Cd–NCS(4)
Identification code	$[Cd(amp)(N_3)_2]_n$	$[Cd(amp)_2(NCS)_2]$
Empirical formula	$C_6H_8CdN_8$	$C_{14}H_{16}CdN_6S_2$
Formula weight	304.60	444.85
Crystal system	Triclinic	Monoclinic
Space group	P-1	P2(1)/n
Unit cell dimensions	$a = 6.5725$ (7) Å	$a = 9.6129$ (6) Å
	$b = 7.9927$ (8) Å	$b = 16.1660$ (11) Å
	$c = 9.9758$ (10) Å	$c = 11.6647$ (7) Å
	$\alpha = 76.395$ (8)°	$\alpha = 90°$
	$\beta = 83.073$ (8)°	$\beta = 97.550$ (7)°
	$\gamma = 85.992$ (8)°	$\gamma = 90°$
Volume	505.16 (9) $Å^3$	1797.0 (2) $Å^3$
Z	2	4
Density (calculated)	2.003 g cm^{-3}	1.644 g cm^{-3}
Absorption coefficient	2.142 mm^{-1}	1.454 mm^{-1}
F(000)	296	888
θ range for data collection	2.11 to 28.99	2.5 to 28.00
Index ranges	$-8 \leq h \leq 8$	$-12 \leq h \leq 12$
	$-10 \leq k \leq 10$	$-20 \leq k \leq 20$
	$-13 \leq l \leq 13$	$-13 \leq l \leq 14$
Reflections collected	9554	11426
Independent reflections	2681 [R(int) = 0.0597]	3869 [R(int) = 0.0335]
Completeness to theta	99.7 %	98.8 %
Data/restraints/parameters	2681/0/137	3869/0/208
Goodness-of-fit on F^2	1.064	0.865
Final R indices [I > 2sigma(I)]	R1 = 0.0191, wR2 = 0.0465	R1 = 0.0252, wR2 = 0.0558
indices (all data)	R1 = 0.0201, wR2 = 0.0470	R1 = 0.0395, wR2 = 0.0578
Largest diff. peak, hole	0.56, −0.73 e $Å^{-3}$	1.63, −0.27 e $Å^{-3}$

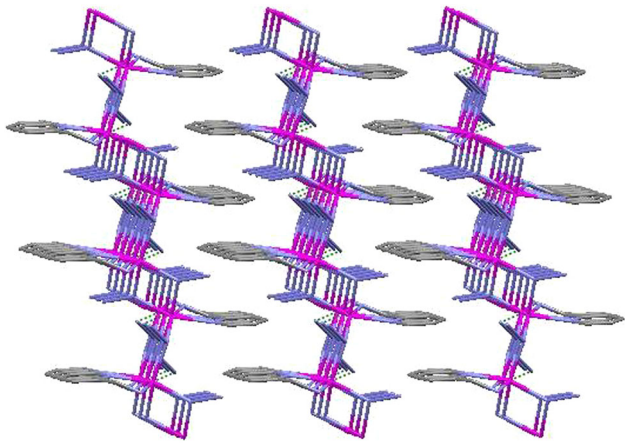

Fig. 7 The packing diagram of compound (**3**)

Table 3 Selected bond lengths/Å and angles/° for **1–2**

Zn–NNN(1)		Zn–NCS(2)	
Zn1–N2^{i}	2.103 (1)	Zn1–N2^{i}	2.109 (1)
Zn1–N2	2.103 (1)	Zn1–N2	2.109 (1)
Zn1–N1	2.154 (1)	Zn1–N1^{i}	2.136 (1)
Zn1–N1^{i}	2.154 (1)	Zn1–N1	2.136 (1)
Zn1–N3	2.281 (1)	Zn1–N3^{i}	2.271 (2)
Zn1–N3^{i}	2.281 (1)	Zn1–N3	2.271 (2)
N2^{i}–Zn1–N2	180.0	N2^{i}–Zn1–N2	180.0
N2^{i}–Zn1–N1	100.54 (5)	N2–Zn1–N1^{i}	101.02 (6)
N2–Zn1–N1	79.46 (5)	N2–Zn1–N1	78.98 (6)
N1–Zn1–N1^{i}	180.0	N1^{i}–Zn1–N1	180.0
N2^{i}–Zn1–N3	90.28 (5)	N2^{i}–Zn1–N3^{i}	91.32 (6)
N2–Zn1–N3	89.72 (5)	N1–Zn1–N3^{i}	91.92 (6)
N1–Zn1–N3	89.13 (5)	N2^{i}–Zn1–N3	88.68 (6)
N1^{i}–Zn1–N3	90.87 (5)	N2–Zn1–N3	91.32 (6)
N2-Zn1–N3^{i}	90.28 (5)	N1–Zn1–N3	88.08 (6)
N3–Zn1–N3^{i}	180.0	N3^{i}–Zn1–N3	180.0

(i) $1-x, 1-y, 1-z$

intermolecular interaction are effective in stabilization of the crystal structure and formation of the 3-D supramolecular complex too. The ORTEP view with numbering scheme for Cd^{II} compounds is shown in Figs. 5, 6. Cu(II) analog of compound **2** is known too, and is isomorphic to **2** [32, 33]. Determination of the structure of compound **3** by X-ray crystallography (Table 2; Figs. 5, 7) showed that in the crystal structure of compound **3**, Cd^{II} is six-coordinate in a configuration by two nitrogen atoms from 2-Aminomethylpyridine ligand and four nitrogen atoms from four N_3^- counter ion. Selected bond lengths/Å and angles/° and hydrogen bonding have been listed in Tables 4 and 6 for compound

Table 4 Selected bond lengths/Å and angles/° for **3–4**

Cd–NNN(3)		Cd–NCS(4)	
Cd1–N6	Cd1–N6	2.304 (2)	2.287 (1)
Cd1–N3	Cd1–N5	2.314 (2)	2.326 (1)
Cd1–N1	Cd1–N4	2.325 (2)	2.334 (1)
Cd1–N2	Cd1–N1	2.357 (2)	2.336 (1)
Cd1–N6^{ii}	Cd1–N3	2.365 (2)	2.416 (1)
Cd1–N3^{i}	Cd1–N2	2.368 (2)	2.428 (1)
N6–Cd1–N3	N6–Cd1–N5	92.47 (9)	99.61 (6)
N6–Cd1–N1	N6–Cd1–N4	162.67 (1)	159.51 (6)
N3–Cd1–N1	N5–Cd1–N4	88.45 (9)	93.32 (6)
N6–Cd1–N2	N6–Cd1–N1	96.50 (9)	99.04 (6)
N3–Cd1–N2	N5–Cd1–N1	90.54 (9)	156.16 (5)
N1–Cd1–N2	N4–Cd1–N1	100.79 (8)	73.44 (5)
N6–Cd1–N6^{ii}	N6–Cd1–N3	90.59 (9)	74.90 (5)
N3–Cd1–N6^{ii}	N5–Cd1–N3	97.10 (9)	91.72 (5)
N1–Cd1–N6^{ii}	N4–Cd1–N3	72.13 (8)	88.97 (5)
N2–Cd1–N6^{ii}	N1–Cd1–N3	169.35 (7)	107.41 (5)
N6–Cd1–N3^{i}	N6–Cd1–N2	86.77 (9)	98.98 (5)
N3–Cd1–N3^{i}	N5-Cd1–N2	161.65 (9)	75.92 (5)
N1–Cd1–N3^{i}	N4–Cd1–N2	97.70 (8)	99.55 (5)
N2–Cd1–N3^{i}	N1–Cd1–N2	71.36 (8)	86.63 (5)
N6^{ii}–Cd1–N3^{i}	N3–Cd1–N2	101.24 (8)	165.28 (6)

(i) $-x, 1-y, 1-z$, (ii) $1-x, 1-y, 1-z$

3 respectively. In the crystal structure of **3**, Fig. 7, intermolecular C–H···N and N–H···N hydrogen bonds (Table 6), π-π interaction between the pyridine rings and other intermolecular interaction are effective in stabilization of the crystal structure and formation of the 3-D supramolecular complex Tables 3 and 5. Selected bond lengths/Å and angles/° and hydrogen bonding have been listed in Table 4. Determination of the structure of compound **4** by X-ray crystallography (Table 2 and Figs. 6, 8) showed that in the crystal structure of compound **4**, Cd^{II} is six-coordinate in a configuration by four nitrogen atoms from 2-Aminomethylpyridine ligand and two nitrogen atoms from two NCS^- counter ion. Selected bond lengths/Å and angles/° and hydrogen bonding have been listed in Tables 4 and 6 for compound **4** respectively. In the crystal structure of **4**, Fig. 8, intermolecular N–H···S and C–H···S hydrogen bonds (Table 6), π-π interaction between the pyridine rings and other intermolecular interaction are effective in stabilization of the crystal structure and formation of the 3-D supramolecular complex two. To examine the thermal stability of compounds **1–4** thermal gravimetric (TG) and differential thermal analyses (DTA) were carried out between 50 and 850 °C under oxygen flow (Figs. 9, 10, 11 and 12). Mass loss calculations are consistent with the correct final

Table 5 Hydrogen bonding and intermolecular interactions for **1–2**

	H···A/Å	B···A/Å	B-H···A/°
Zn-NNN(1)			
N2–H2B···N3 (1−*x*, 1/2+*y*, 1/2−*z*)	2.231 (1)	3.066 (2)	152.40
N2–H2A···N5 (*x*, 1/2−*y*, −1/2+*z*)	2.344 (2)	3.233 (2)	130.99
C3–H3···N5 (2−*x*, 1/2+*y*, 3/2−*z*)	2.635 (2)	3.302 (2)	128.40
C1–H1···N4 (*x*, 1/2−*y*, 1/2+*z*)	2.701 (2)	3.569 (2)	153.93
π-π stacking (slipped face-to-face)	–	3.286 (2)	–
C6–H6B···Cg (C1···N1) (*x*, 1/2−*y*, −1/2+*z*)	–	2.614 (2)	–
Zn-NCS(2)			
N2–H2B···N3 (1−*x*, 1/2+*y*, 1/2−*z*)	2.432 (2)	3.220 (2)	145.01
N2–H2A···S1 (*x*, 1/2−*y*, −1/2+*z*)	2.664 (6)	3.515 (2)	156.05
C2–H2···S1 (2−*x*, 1/2+*y*, 1/2−*z*)	2.908 (2)	3.628 (2)	134.33
π-π stacking (slipped face-to-face)	–	3.455 (3)	–

Table 6 Hydrogen bonding and intermolecular interactions for **3–4**

	H···A/Å	B···A/Å	B–H···A/°
Cd–NNN(3)			
N2–H2B···N5 (*x*, −1+*y*, *z*)	2.194 (2)	3.113 (2)	177.01
N2–H2A···N5 (1−*x*, 1−*y*, 1−*z*)	2.353 (2)	3.159 (2)	146.21
C6–H6B···N8 (1−*x*, −*y*, 1−*z*)	2.582 (2)	3.358 (3)	135.06
C2–H2···N8 (*x*, 1+*y*, −1+*z*)	2.576 (2)	3.407 (2)	146.22
C4–H4···N8 (*x*, *y*, −1+*z*)	2.574 (2)	3.516 (3)	170.88
π-π stacking (slipped face-to-face)	–	3.234	–
π-π stacking (slipped face-to-face)	–	3.320	–
Cd–NCS(4)			
N4–H4A···S2 (1/2+*x*, 1/2−*y*, 1/2+*z*)	2.554 (8)	3.461 (2)	175.43
N2–H2A···S1 (−1/2+*x*, 1/2−*y*, −1/2+*z*)	2.625 (7)	3.525 (2)	170.70
N4–H4B···S1 (3/2−*x*, −1/2+*y*, 3/2−*z*)	2.7805 (7)	3.523 (2)	139.55
C4–H4···S2 (1/2−*x*, −1/2+*y*, 3/2−*z*)	2.9102 (7)	3.699 (3)	142.27
N2–H2B···S1 (3/2−*x*, −1/2+*y*, 3/2−*z*)	2.9220 (8)	3.456 (2)	119.00
π-π stacking (slipped face-to-face)	–	3.520	–

decomposition product to be ZnO. The DTA curve displays four distinct endothermic peaks at 80, 130, 150 and 240 °C as well as four exothermic peaks at 100, 140, 200, and 280 °C (Fig. 9). Compound **2** is stable up to 140 °C, at which decomposition begins. Mass loss calculations are consistent with the correct final decomposition product to be ZnO. The DTA curve displays two distinct endothermic peaks at 240 and 330 °C as well as two exothermic peaks at 200 and 300 °C (Fig. 10). Compound **3** is stable up to 200 °C, at which decomposition begins. Mass loss calculations are consistent with the correct final decomposition product to be CdO (Fig. 11). Compound **4** is stable up to 180 °C, at which decomposition begins. Mass loss calculations are consistent with the correct final decomposition product to be CdO (Fig. 12). ZnO and CdO nano-particles were synthesized from the decomposition of the precursors **1–4** in 600 °C under air atmosphere for 4 h. The morphology and size of the as-prepared ZnO and CdO samples were further investigated using SEM (Fig. 13). SEM images of the residue which are obtained from the direct calcination of compounds show the formation of zinc(II) and cadmium(II) oxide nanoparticles with a diameter distribution of 60–70 and 50–60 nm at 600 °C respectively. The final product from thermolysis of compounds **1–2** is based on their XRD patterns, hexagonal ZnO. The phase purity of the as-prepared hexagonal ZnO nano-particles are completely obvious and all diffraction peaks are perfectly indexed to

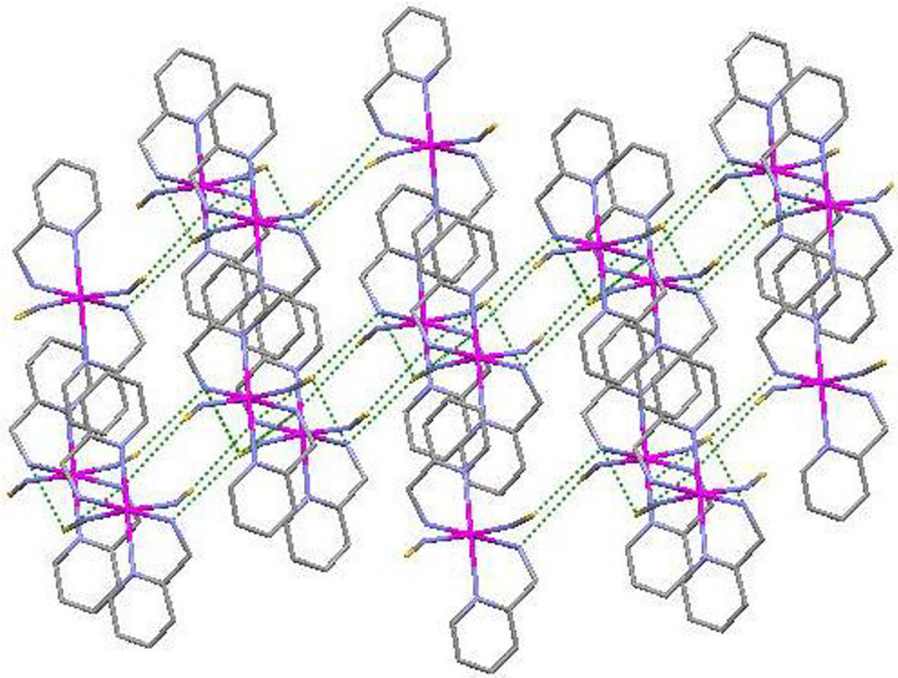

Fig. 8 The packing diagram of compound (**4**)

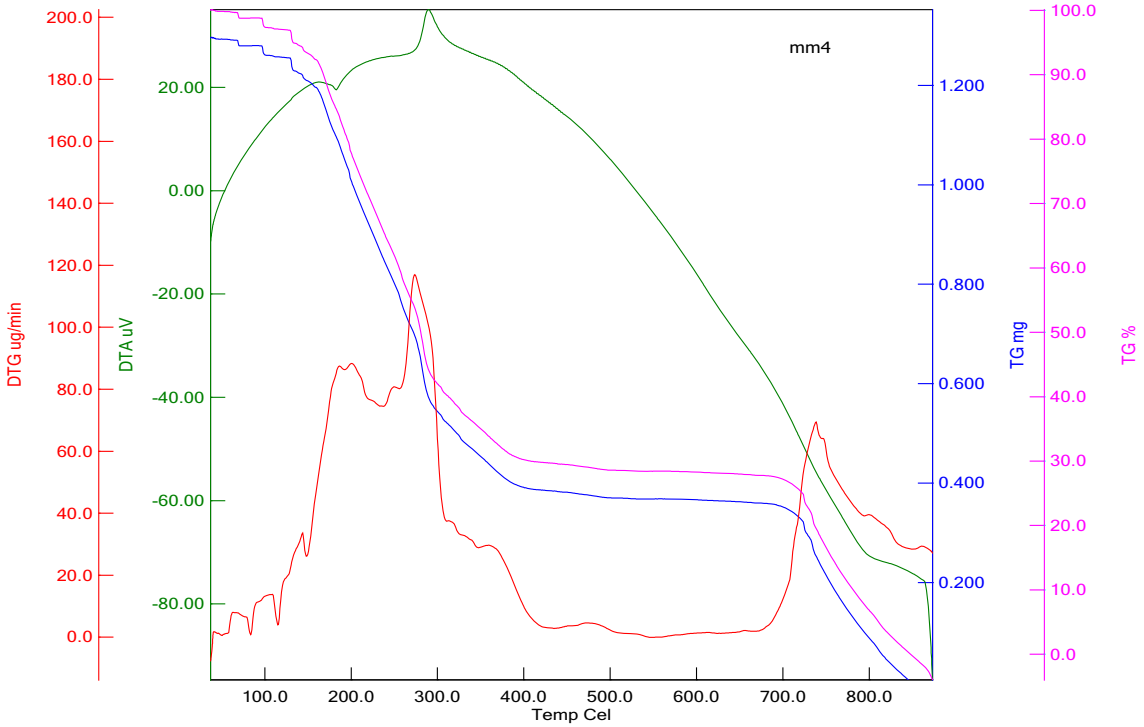

Fig. 9 TG-DTG diagram of compound (**1**)

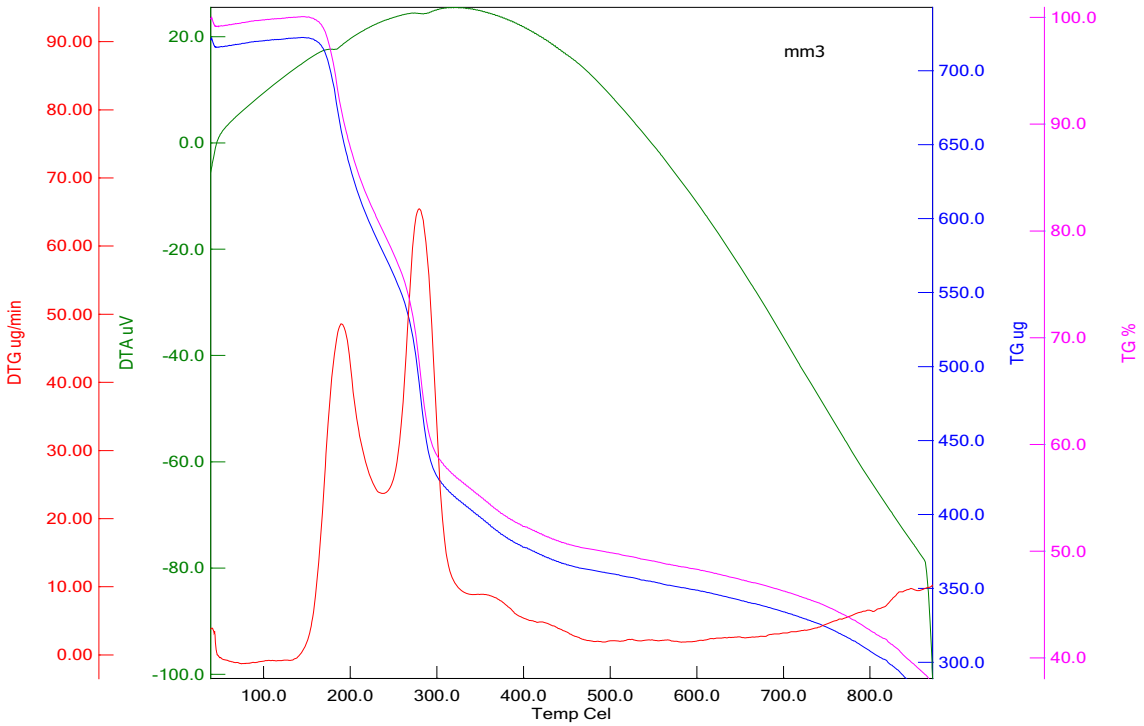

Fig. 10 TG-DTG diagram of compound (**2**)

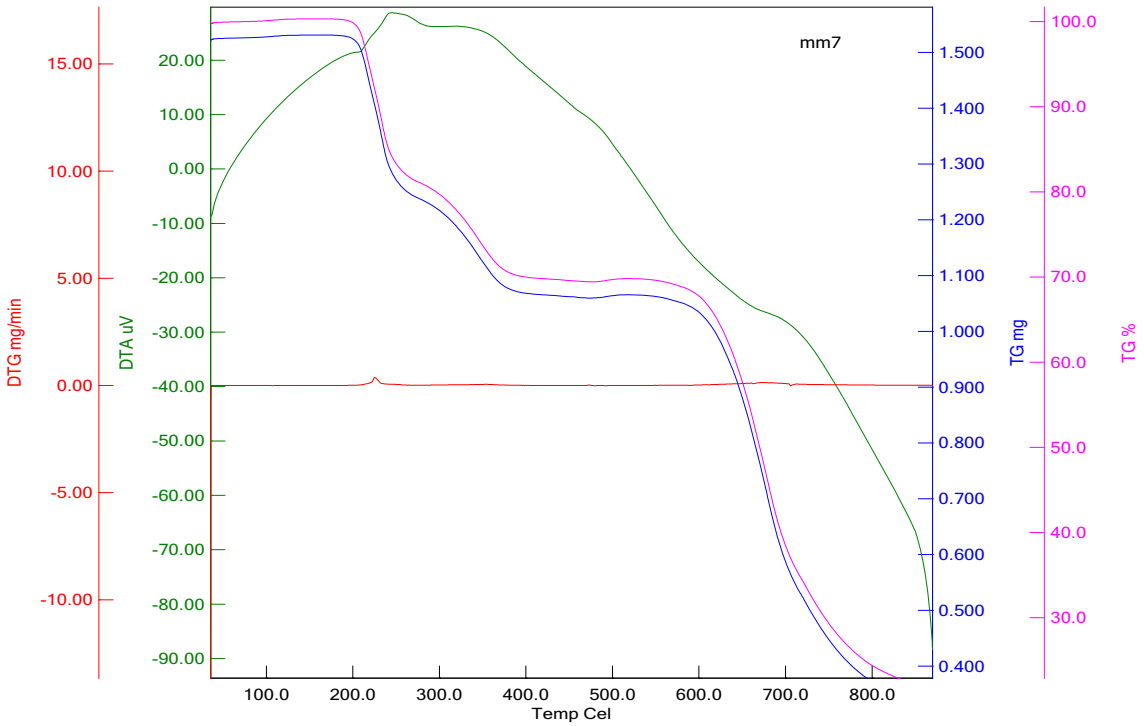

Fig. 11 TG-DTG diagram of compound (**3**)

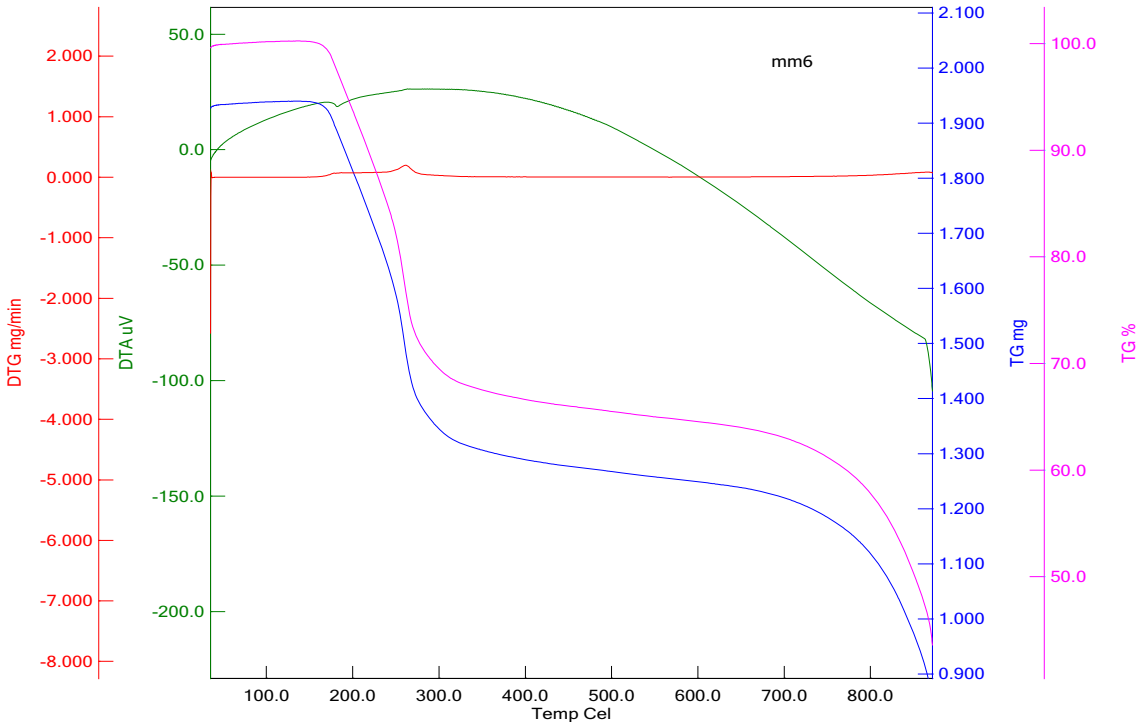

Fig. 12 TG-DTG diagram of compound (**4**)

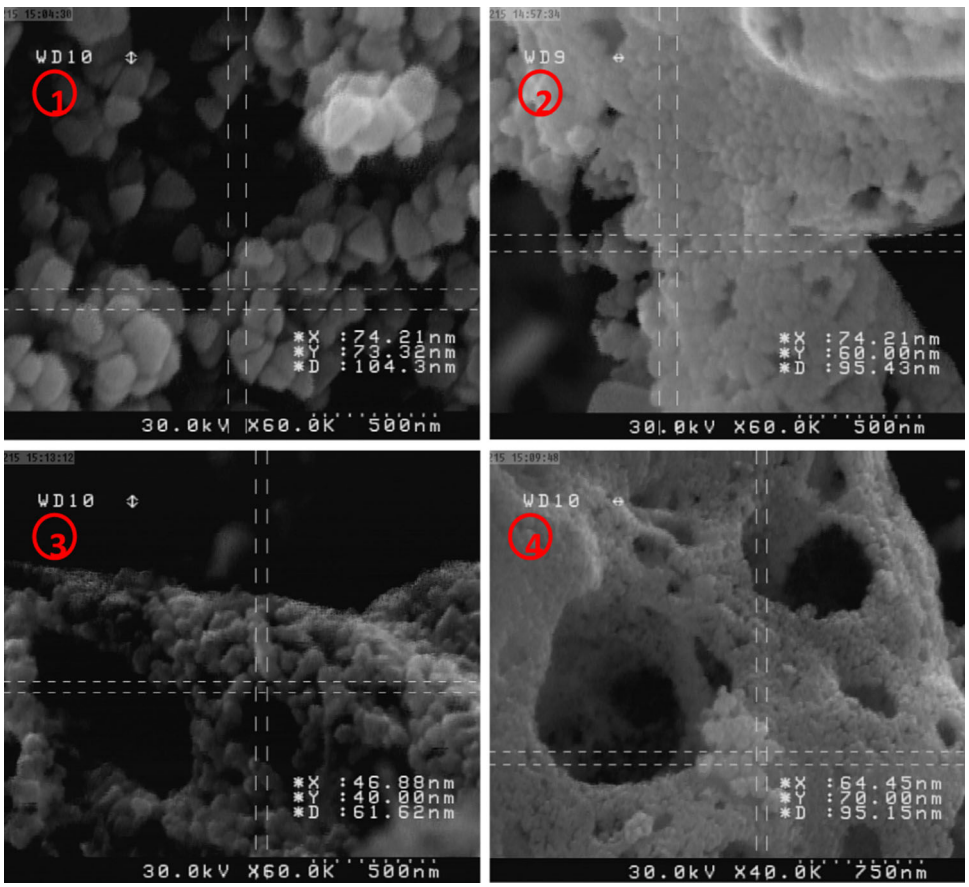

Fig. 13 SEM image of ZnO nanostructure prepared by thermal decomposition of compound **1–2** (*up*) and CdO nanostructure prepared by thermal decomposition of compound **3–4** (*down*) at 600 °C

the hexagonal ZnO structure with the lattice parameters of a = 3.24982 Å, c = 5.20661 Å, Z = 2 and S.G = $P6_3mc$ which are in JCPDS card file no. 36-1451. No characteristic peaks of impurities are detected in the XRD pattern (Fig. 14). Figure 15 provides the XRD pattern of the residue obtained from calcination of compound **3, 4**. The obtained pattern matches with the standard pattern of Monteponite cadmium(II) oxide with the lattice parameters (a = 4.6953 Å, S.G. = Fm3m and z = 4) which is the same as the reported values (JCPDS card no. 05-0640).

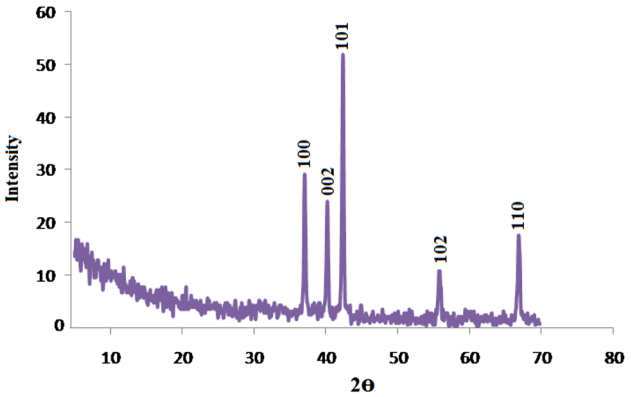

Fig. 14 X- ray powder diffraction pattern of ZnO produced by thermolyses of compounds **1–2**

4 Conclusion

In summary four new Zn(II) and Cd(II) coordination polymer, $[Zn(2\text{-}AMP)_2(N_3)_2]_n$ (**1**), $[Zn(2\text{-}AMP)_2(SCN)_2]_n$ (**2**), $[Cd(2\text{-}AMP)(N_3)_2]_n$ **(3)** and $[Cd(2\text{-}AMP)_2(SCN)_2]_n$ **(4)** {2-AMP: 2-Aminomethylpyridine}, have been synthesized and characterized by single crystal X-ray diffraction. Small and spherical ZnO and CdO particles with good separation were produced by thermolysis of compounds **1–4** at 600 °C. This study demonstrates the Zinc(II) and Cadmium(II) complexes may be suitable precursors for the preparation of nanoscale materials and it does not need special conditions like high temperature, long times and pressure controlling [34–37].

5 Supplementary Material

Crystallographic data for the structures reported in the paper has been deposited with the Cambridge Crystallographic Data Centre as supplementary publication no, CCDC-1446410-1446413 for compounds **1–4** respectively. Copies of the data can be obtained on application to CCDC, 12 Union Road, Cambridge CB2 1EZ, UK [Fax: +44–1223/336033; e–mail: deposit@ccdc.cam.ac.uk].

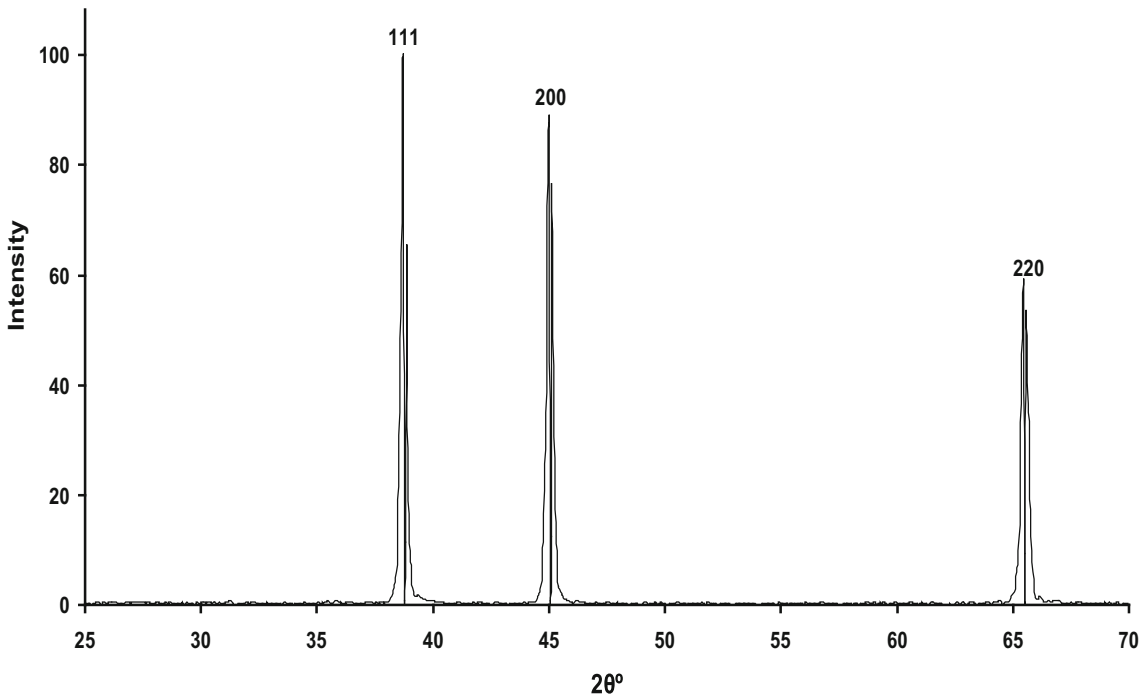

Fig. 15 X- ray powder diffraction pattern of CdO produced by thermolyses of compounds **3–4**

Acknowledgments Support of this investigation by Tarbiat Modares University and Payame Noor University, are gratefully acknowledged.

References

1. A. Morsali, M.Y. Masoumi, Coord. Chem. Rev. **253**, 1882 (2009)
2. G.K.H. Shimizu, G.D. Enright, C.I. Ratcliffe, K.F. Preston, J.L. Reid, J.A. Ripmeester, Chem. Commun. **1485**, 82 (1999)
3. B. Moulton, M.J. Zawartko, Chem. Rev. **101**, 1629 (2001)
4. R. Kitaura, K. Fujimoto, S. Noro, M. Kondo, S. Kitagawa, Angew. Chem. Int. Ed. **41**, 133 (2002)
5. M. Oh, C.A. Mirkin, Nature **438**, 651 (2005)
6. G. Mahmoudi, A. Morsali, A.D. Hunter, M. Zeller, CrystEngComm **9**, 704 (2007)
7. S.R. Batten, S.M. Neville, D.R. Turner, *Coordination polymer: design, analysis and application*, Illustrated edn. (Royal Society of Chemistry, Science Park Cambridge, 2009)
8. A.Y. Robin, K.M. Fromm, Coord. Chem. Rev. **250**, 2127 (2006)
9. A. Aslani, A. Morsali, M. Zeller, Dalton Trans. **38**, 5173 (2008)
10. J. Zhou, Y.Z. Yuan, X. Liu, D.Q. Li, Z. Zhou, Z.-F. Chen, K.-B. Yu, J. Coord. Chem. **59**, 1477 (2006)
11. H.T. Shi, L.M. Qi, J.M. Ma, H.M. Cheng, J. Am. Chem. Soc. **125**, 3450 (2003)
12. H. Zhang, D.R. Yang, D.S. Li, X.Y. Ma, S.Z. Li, D.L. Que, Cryst. Growth Des. **5**, 547 (2005)
13. D.B. Kuang, A.W. Xu, Y.P. Fang, H.Q. Liu, C. Frommen, D. Fenske, Adv. Mater. **15**, 1747 (2003)
14. L. Hashemi, A. Morsali, Ultrason. Sonochem. **24**, 146 (2015)
15. A. Ennaoui, M. Weber, R. Scheer, H.J. Lewerenz, Sol. Energy Mater. Sol. Cells **54**, 277 (1998)
16. J. Liqiang, W. Baiq, X. Baifu, L. Shudan, S. Keying, C. Weimin, F. Honggang, J. Solid State Chem. **177**, 4221 (2004)
17. V.R. Shinde, T.P. Gujar, C.D. Lokhande, Sens. Actuators B **120**, 551 (2007)
18. S.K.N. Ayudhya, P. Tonto, O. Mekasuwandumrong, V. Pavarajarn, P. Praserthdam, Cryst. Growth Des. **6**, 2446 (2006)
19. M. Vafaee, M.S. Ghamsari, Mater. Lett. **61**, 3265 (2007)
20. Y.S. Kim, W.P. Tai, S.J. Shu, Thin Solid Films **491**, 153 (2005)
21. J.Z. Liu, P.X. Yan, G.H. Yue, L.B. Kong, R.F. Zhuo, Mater. Lett. **60**, 3471 (2006)
22. Y. He, J. Wang, Mater. Lett. **62**, 1379 (2008)
23. P.X. Gao, Z.L. Wang, Appl. Phys. Lett. **84**, 2883 (2004)
24. L. Vayssieres, Adv. Mater. **15**, 464 (2003)
25. C.H. Liu, J.A. Zapien, Y. Yao, X.M. Meng, C.S. Lee, S.S. Fan, Y. Lifshitz, S.T. Lee, Adv. Mater. **15**, 838 (2003)
26. H. Zhang, X.Y. Ma, J. Xu, J. Niu, D. Yang, Nanotechnology **14**(4), 423 (2003)
27. F. Bigdeli, A. Morsali, Mater. Lett. **64**, 4 (2010)
28. R. Jayakrishnan, G. Hodes, Thin Solid Films **440**, 19 (2003)
29. M. Ristic, S. Poporic, S. Music, Mater. Lett. **58**, 2494 (2004)
30. L.J. Farrugia, Ortep-3 for Windows. J. Appl. Cryst. **30**, 565 (1997)
31. Mercury 1.4.1, Copyright Cambridge Crystallographic Data Centre, 12 Union Road, Cambridge, CB2 1EZ, UK, 2001–2005
32. N.K. Karan, K.-T. Chan, H.M. Lee, Acta Crystallogr. Sect. E **65**, m525 (2009)
33. M. Shukla, N. Srivastava, S. Saha, T.R. Rao, S. Sunkari, Polyhedron **30**, 754 (2011)
34. F. Marandi, L. Hashemi, A. Morsali, H. Krautscheid, Ultrason. Sonochem. **32**, 86 (2016)
35. M.Y. Masoomi, A. Morsali, Ultrason. Sonochem. **28**, 240 (2016)
36. L. Hashemi, A. Morsali, P. Retailleau, Inorg. Chim. Acta **367**, 207 (2011)
37. F. Molaei, F. Bigdeli, A. Morsali, J. Ind. Eng. Chem. **24**, 229 (2015)